

Pathogenesis and characteristics of large ameloblastoma of the jaw: a report of two rare cases

Journal of International Medical Research

49(5) 1–12

© The Author(s) 2021


Article reuse guidelines:

sagepub.com/journals-permissions

DOI: 10.1177/03000605211014803

journals.sagepub.com/home/imr



Xue Qiao^{1,2,*}, Xing Niu^{3,4,*}, Jiayi Liu³,
Lijie Chen^{3,4}, Yan Guo^{1,2} and Ming Zhong^{3,4} 

Abstract

Ameloblastoma is a common odontogenic epithelial tumor that exhibits various biological behaviors, ranging from simple cystic expansion to aggressive solid masses characterized by local invasiveness, a high risk of recurrence, and even malignant transformation. We report on two cases of unusually large solid ameloblastomas. We detected epithelial–mesenchymal transition-related gene expression and *HRAS* gene single nucleotide polymorphisms, providing possible molecular evidence of mesenchymal morphological changes in ameloblastoma. The detailed analysis of the pathogenesis of these two cases of ameloblastoma may deepen our understanding of this rare disease and offer promising targets for future targeted therapy.

Keywords

Ameloblastoma, epithelial–mesenchymal transition, single nucleotide polymorphism, *HRAS*, gene expression, tumor size

Date received: 1 October 2020; accepted: 12 April 2021

¹Department of Central Laboratory, School and Hospital of Stomatology, China Medical University, Liaoning Province Key Laboratory of Oral Disease, Shenyang, Liaoning, China

²Department of Oral Biology, School and Hospital of Stomatology, China Medical University, Liaoning Province Key Laboratory of Oral Disease, Shenyang, Liaoning, China

³Department of Oral Histopathology, School and Hospital of Stomatology, China Medical University, Liaoning Province Key Laboratory of Oral Disease, Shenyang, Liaoning, China

⁴Department of Stomatology, Xiang'an Hospital of Xiamen University, Xiamen, Fujian, China

*These authors contributed equally to this study.

Corresponding author:

Ming Zhong, Department of Stomatology, Xiang'an Hospital of Xiamen University, No. 2000 Xiang'an East Road, Xiang'an District, Xiamen, Fujian 361102, China. Email: mzhong@cmu.edu.cn



Introduction

Ameloblastoma is one of the most common and clinically important odontogenic tumors. Ameloblastomas are thought to derive from epithelial tissues associated with tooth formation, including the enamel organ, the epithelial cell rests of Malassez, the reduced enamel epithelium, and the lining of odontogenic cysts.^{1,2} Ameloblastomas comprise several types, including conventional ameloblastoma, and peripheral/extraosseous and unicystic types.³ Most ameloblastomas are conventional ameloblastomas and are thought to be histologically benign but locally aggressive; however, malignant transformation and recurrence have been observed in some cases,^{4,5} with complete surgical removal of the tumor and the tumor-free margins being the most effective treatment strategy.^{6,7} If they are not surgically removed, these tumors can continue to grow to become very large.

Epithelial–mesenchymal transition (EMT) is a complex process that enables dynamic changes in cells from an epithelial to a mesenchymal morphology. EMT plays a pivotal role in mediating the migratory and invasive capabilities of many tumor cell types.⁸ Moreover, several studies of ameloblastomas have reported EMT-related gene transcription changes,^{9,10} suggesting a possible role for EMT in the development and progression of ameloblastoma. Multiple factors, including gene mutations, are involved in the tumorigenesis and tumor progression of ameloblastoma, and mutations in several oncogenes, such as B-type Raf kinase (*BRAF*) and smoothened (*SMO*) have been reported.^{11–13} Genome-wide sequencing of single nucleotide polymorphisms (SNPs) allows the detection of all possible gene polymorphisms in one chip, and has been widely used to identify possible genetic markers in different tumor types.

In the present study, we detail two patients with very large, solid ameloblastomas, reported in accordance with the CARE guidelines.^{14–16} We detected the expression levels of several important EMT-related proteins and showed evidence of mesenchymal morphological changes in ameloblastoma tissues. We also searched for possible downstream target genes by examining SNPs in long-growing ameloblastoma tumors, and additionally assessed the current tumors for the presence of these cancer-associated SNPs.

Case Presentation

Case 1

A 51-year-old female patient presented with a large swelling of the jaw that had been present for 17 years. Over this time, the patient had gradually lost sensation in her lips on the left side and had difficulty eating because of her limited ability to open her mouth, at which time she presented at the hospital for treatment. Examination revealed a 16- × 12-cm extra-oral swelling in the left buccal mandible region (Figure 1a, b). An intra-oral swelling involving the lower-left tongue, left buccal facial region, and left maxilla region was also observed. Radiographic imaging revealed multiple radiolucent lesions that appeared as mixtures of cystic and solid tissues with significant liquid transudation (Figure 1c). The intra-oral cavity and the basis cranii were also impacted because of the complexity of the anatomical structures and the large tumor size.

Case 2

A 22-year-old man who had been referred for clinical treatment presented with a large protruding mass in the central portion of the left facial region. The mass had developed over the preceding 10 years.

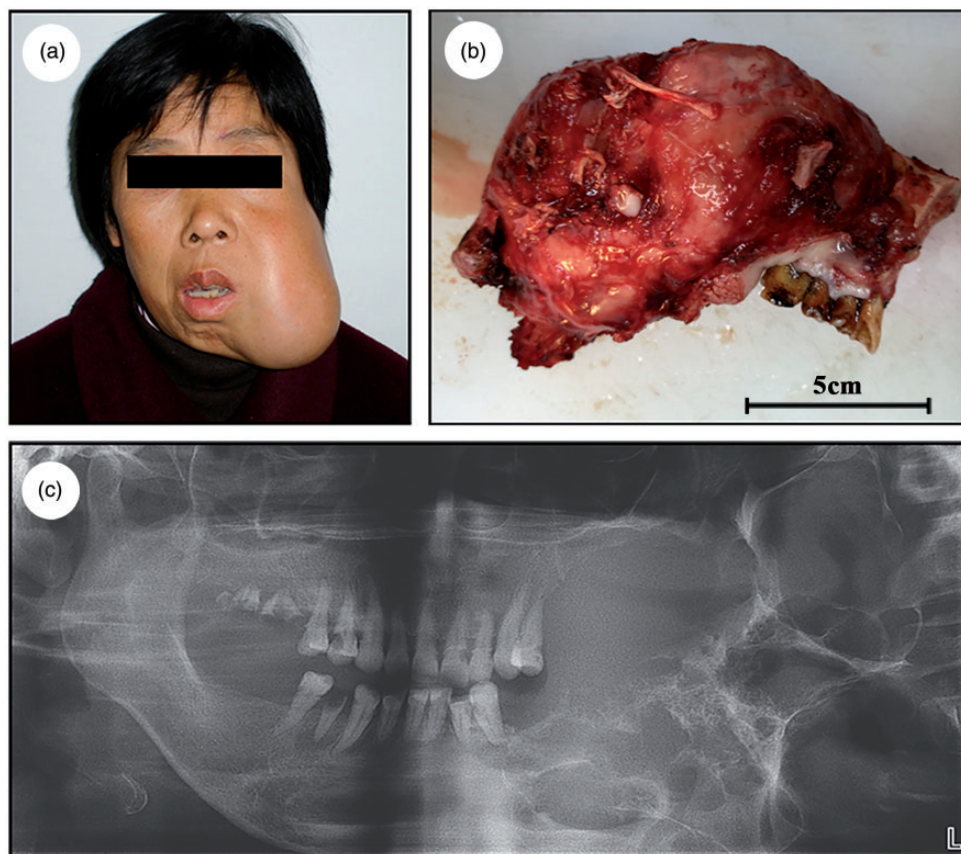


Figure 1. Case I. (a) Photograph of the patient showing tumor involving the lower left oral cavity, and left buccal facial and maxilla regions. (b) Resected tumor. (c) X-ray image showing a large tumor in the left mandible with many radiolucent lesions.

The patient complained of pain emanating from the back teeth on his left side. Extra-oral examination revealed an obvious swelling in the left lower facial region, including the maxilla and the mandible, and intra-oral examination revealed the involvement of nearly half of the jaw, including the mandibular first and second molars (Figure 2a, b). Computed tomography scanning was carried out to measure the largest dimensions of the tumor (Figure 2c, d).

We obtained patient consent for treatment, and the patients provided written informed consent for publication of this report. The study complied with the

relevant CARE guidelines and was conducted in a manner consistent with the Declaration of Helsinki.

Histologic/microscopic findings

The tumors were surgically resected, fixed using 10% neutral-buffered formalin, paraffin embedded, decalcified using 10% formic acid, and cut into 4- μ m-thick sections for hematoxylin and eosin (H&E) staining. Histopathologically, H&E staining revealed heterogeneous growth changes due to the long-term growth of the ameloblastoma in both cases. Multiple sampling

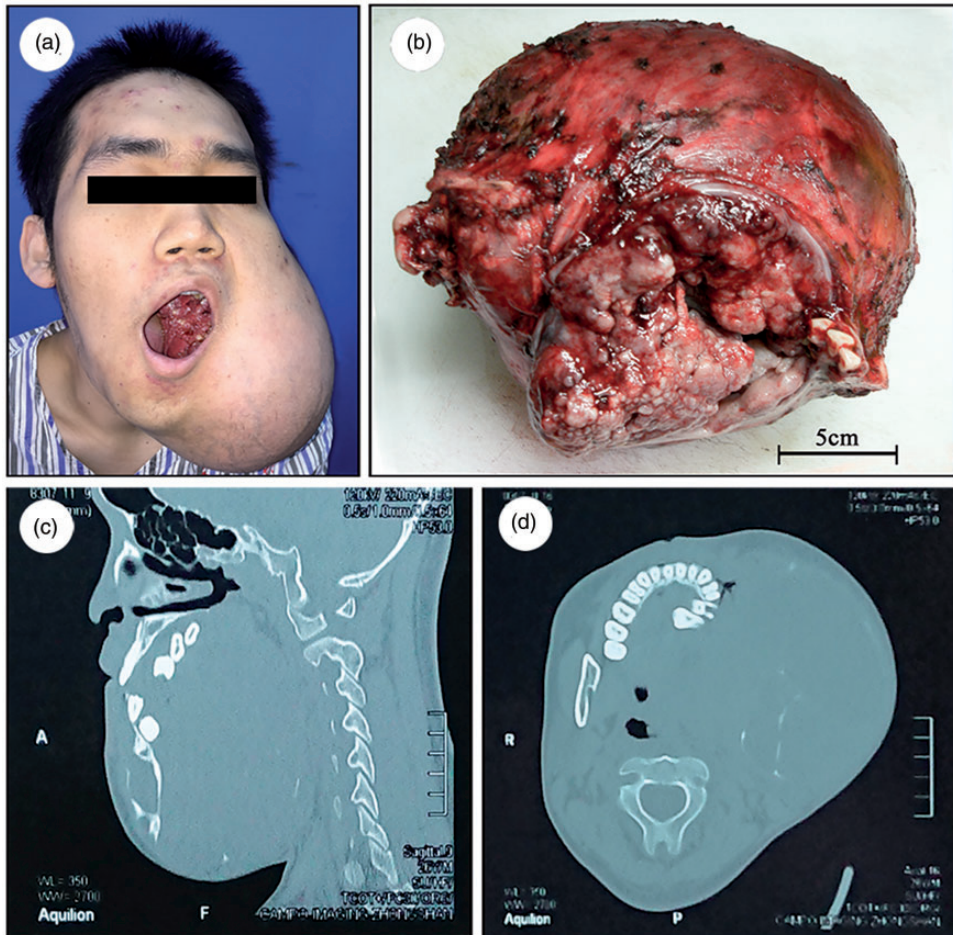


Figure 2. Case 2. (a) Photograph of the patient showing tumor involving the lower left tongue, and left buccal facial and maxilla regions. (b) Resected tumor. (c, d) Computed tomography images showing a large light-transmission area of the tumor in the mandible with extensive bony destruction, cortical thinning, expansion, and perforation of the left buccal and lingual mandible.

revealed squamous metaplasia (Figure 3a, b), dense cell growth, deep nuclear staining (Figure 3c, d), granular degeneration (Figure 3e), and intracellular hyalinization in some regions of the ameloblastoma (Figure 3f).

Immunohistochemical analysis

Tissue sections prepared as above were deparaffinized using xylene, followed by

rehydration through graded ethanols. Endogenous peroxidase activity in the samples was then quenched using methanol containing 0.3% H_2O_2 for 30 minutes, followed by microwaving in citrate phosphate buffer (pH 6.0) to facilitate antigen retrieval. Slides were then probed overnight using appropriate polyclonal antibodies (1:1000) at 4°C, followed by secondary antibodies (1:5000) for 2 hours at room temperature. The primary antibodies used were specific

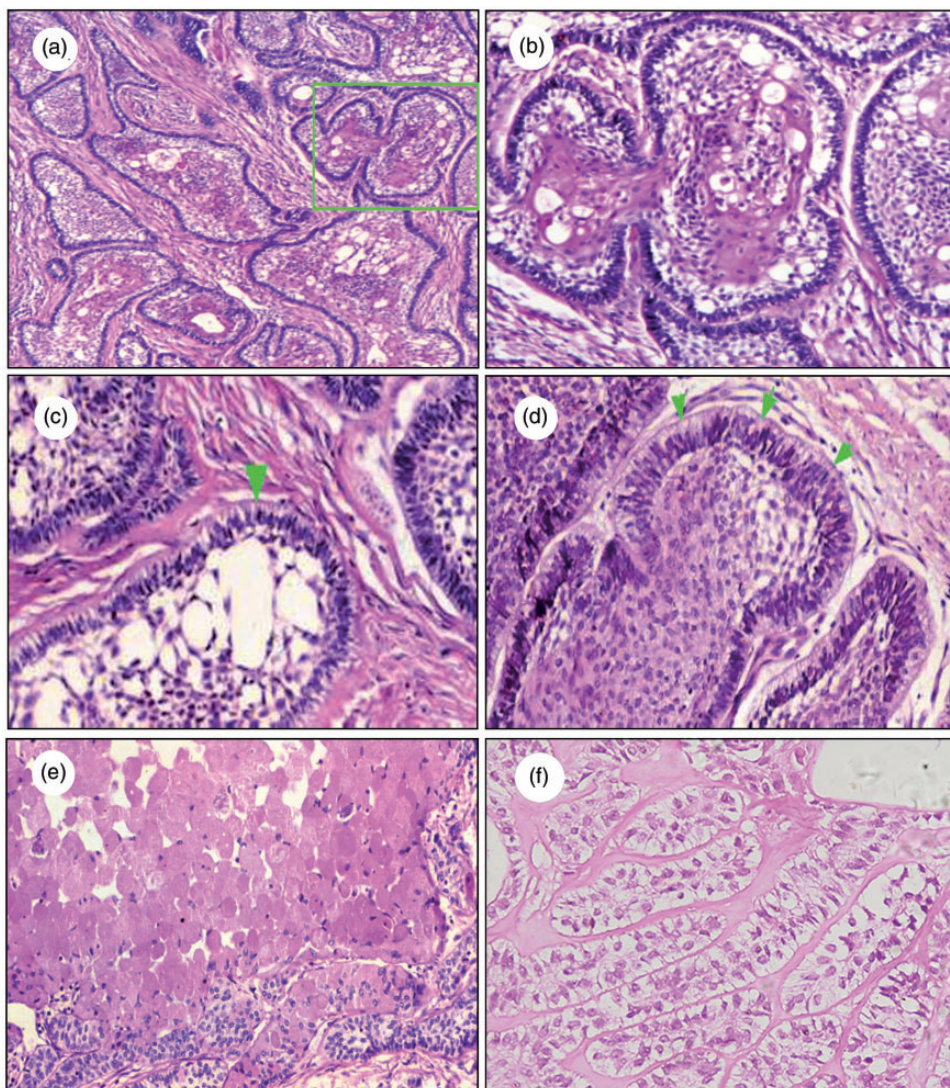


Figure 3. Hematoxylin and eosin staining of tumor samples from both cases. (a) Isolated epithelial mass distributed in the mature connective tissue stroma with squamous metaplasia in the stellate reticular layer. Magnification $\times 100$. (b) Stellate reticular cells were polygonal, similar to the tooth germ layer, accompanied by squamous metaplasia. Magnification $\times 200$. (c, d) The nuclei in the peripheral layer in ameloblastoma tissue were arranged in a palisade shape, and were located far from the basement membrane (green arrows). Magnification $\times 200$. (e, f) Granular degeneration and intracellular hyalinization occurred in some areas. Magnification $\times 100$.

for Ki-67, cytokeratin (CK) 8/18, CK19, CK7, N-cadherin, E-cadherin, and vimentin (all from Abcam, MA, USA). Polyclonal secondary anti-rabbit and

anti-mouse antibodies were from Santa Cruz Biotechnology (Dallas, TX, USA) and Abbkine (Wuhan, China), respectively. The immunohistochemical staining results

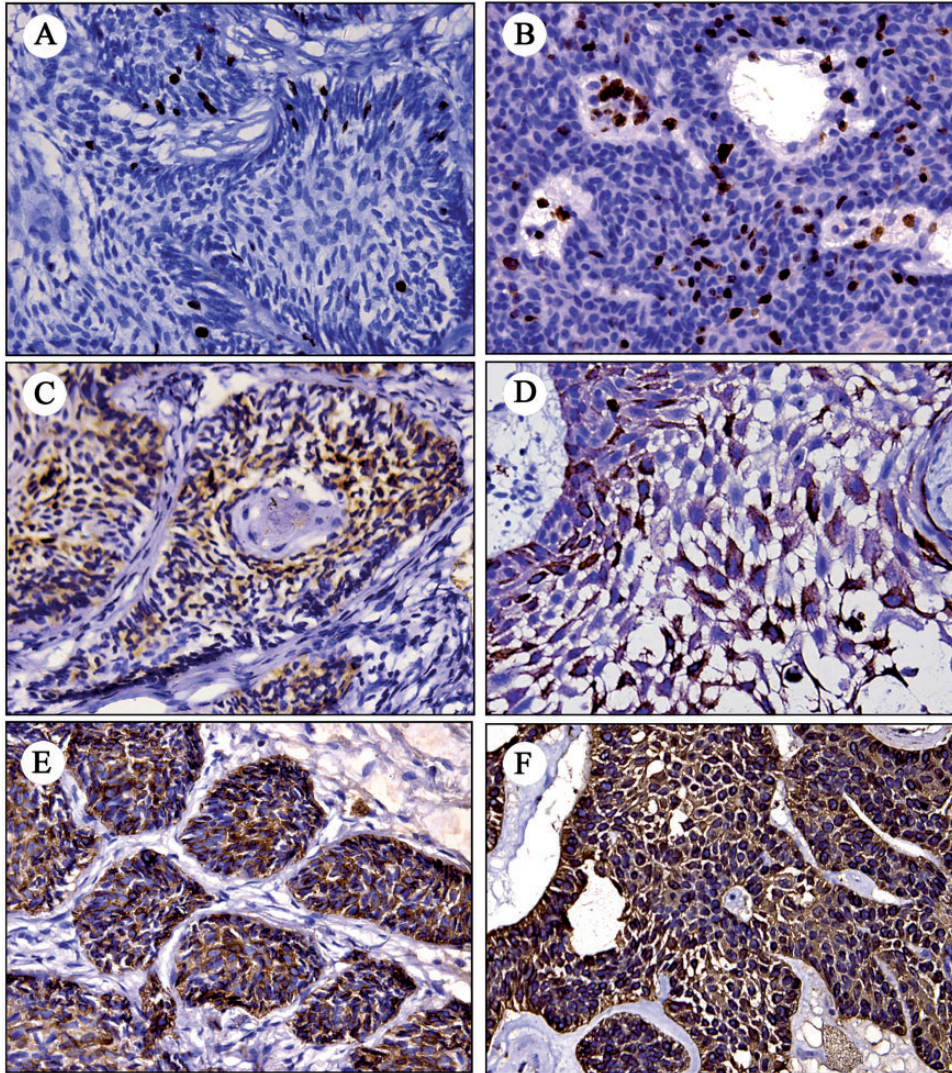


Figure 4. Immunohistochemistry staining of tumor samples from both cases. (a) Case 1 and (b) Case 2 showed positive expression of Ki-67 in the nuclei in the peripheral and stellate reticular layers in ameloblastoma tissue. (c) Case 1 and (d) Case 2 showed cytokeratin (CK) 8/18 expression in the cytoplasm of the peripheral and stellate reticular layers in adenoblastoma tissue (Streptomyces-peroxidase reaction $\times 200$). (e) Case 1 and (f) Case 2 showed positive CK19 expression in the cytoplasm of the peripheral and stellate reticular layers in adenoblastoma tissue with Streptomyces-peroxidase reaction $\times 400$.

revealed that both tumors were positive for Ki-67 in the nucleus in cells in the peripheral and stellate reticular layers (Figure 4a, b). CK8/18 and CK19 were strongly expressed in the cytoplasm in the peripheral and stellate reticular layers (Figure 4c-f).

Both cases were negative for CK7 expression (not shown).

Previous research has suggested that ameloblastomas can exhibit aggressive local growth.¹⁷ Consistent with this, surgical resection indicated clear signs of

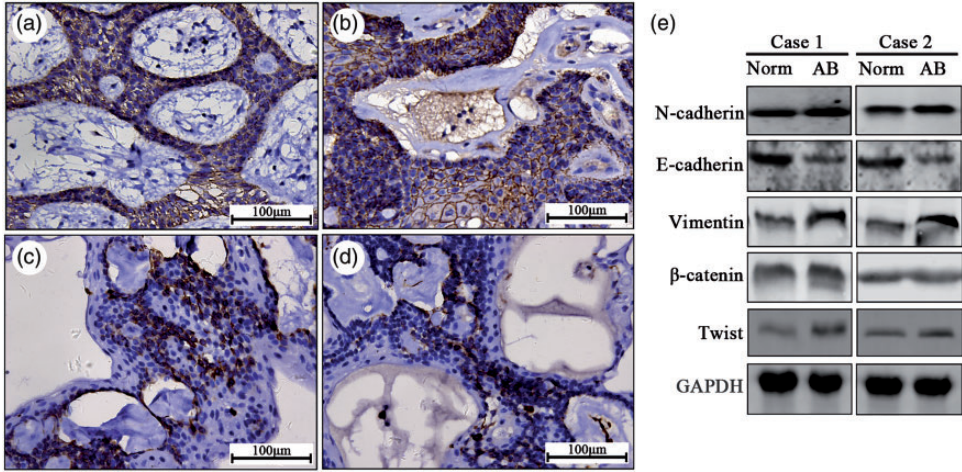


Figure 5. Detection of epithelial–mesenchymal transition (EMT)-related proteins in both cases. Positive staining of N-cadherin in cytoplasm of stellate reticular and peripheral layers in ameloblastoma tissues in (a) Case 1 and (b) Case 2 (Streptomyces-peroxidase reaction $\times 200$). Positive vimentin staining in cytoplasm of stellate reticular layer and nuclei of the lenticular layer in (c) Case 1 and (d) Case 2 with SP $\times 200$. (e) EMT-related proteins including N-cadherin, E-cadherin, vimentin, β -catenin and Twist were positively expressed in tumor tissues as shown by western blot. GAPDH, glyceraldehyde 3-phosphate dehydrogenase.

aggressive growth and bone destruction in both the current patients. We also looked for signs of EMT in the ameloblastomas, given that EMT plays a key role in mediating the migratory and invasive capabilities of many tumor cell types. To that end, we assessed the expression levels of N-cadherin and vimentin using immunohistochemistry. N-cadherin was strongly expressed in the cytoplasm of the ameloblastoma stellate reticular and peripheral layers (Figure 5a, b), and vimentin was strongly expressed in the cytoplasm of cells in the stellate reticular layer and in the nuclei in the lenticular layer (Figure 5c, d). We also detected EMT-related biomarkers by western blot, and found higher expression levels β -catenin, Twist, N-cadherin, and vimentin proteins and lower levels of E-cadherin in tumors, indicating that EMT was activated in ameloblastoma tissues compared with the tumor-free margins (Figure 5e).

Genome-wide SNP sequencing

To gain further insight into the molecular mechanisms underlying the development of these large ameloblastomas, we conducted genome-wide SNP sequencing of both tumors, with the aim of identifying gene mutations associated with ameloblastoma development. We collected blood samples from both patients before surgery and subjected the samples to immediate SNP analysis. The genomic DNA samples were fragmented by sonication, followed by end repair and the addition of adapters to both ends of each fragment. This bar-coded library was then mixed with biotinylated RNA library baits and magnetic beads to target specific regions for use with the Agilent SureSelect Human All Exon V6 Kit (Agilent Technologies Inc., Santa Clara CA USA). After capturing, the sequences were amplified prior to 150-bp paired-end sequencing using an Illumina Hi Seq X Ten system (Illumina,

Table 1. Detection of *HRAS* gene single nucleotide polymorphisms in two patients with ameloblastoma.

Gene ID	Chr	Position	Ref	Alt	Structure type	Mutation type	Case 1	Case 2	
<i>HRAS</i>	11	533854	G	A	–	exonic	nonsynonymous SNV	✓	
		533839	G	A	rs749674880	exonic	nonsynonymous SNV		✓
		534197	C	T	rs41258054	intronic	–		✓
<i>AHNAK</i>	11	62525663	C	T	–	exonic	synonymous SNV	✓	
		62518433	C	T	–	exonic	synonymous SNV		✓
<i>HIP1</i>	7	75542873	G	T	–	exonic	synonymous SNV	✓	
		75558317	A	G	rs7806452	intronic	–		✓
<i>SIRPA</i>	20	1915338	C	A	rs17855615	exonic	nonsynonymous SNV		✓
		1921642	C	T	rs376873084	exonic	synonymous SNV	✓	
<i>DNAJA3</i>	16	4434395	A	T	–	exonic	nonsynonymous SNV		✓
		4444676	G	A	–	exonic	nonsynonymous SNV	✓	
<i>ARHGEF17</i>	11	73311528	G	A	–	exonic	nonsynonymous SNV		✓
		73355870	C	T	–	exonic	nonsynonymous SNV	✓	
<i>MUC3A</i>	7	100960331	G	T	–	exonic	nonsynonymous SNV		✓
		100959872	G	A	–	exonic	nonsynonymous SNV	✓	
<i>BTBD11</i>	12	107520606	G	A	–	exonic	nonsynonymous SNV		✓
		107618169	G	A	–	exonic	nonsynonymous SNV	✓	
<i>PLIN4</i>	19	4512371	C	T	–	exonic	nonsynonymous SNV	✓	
		4513646	G	A	–	exonic	nonsynonymous SNV		✓
<i>VPS37D</i>	7	73671250	G	T	–	exonic	nonsynonymous SNV		✓
		73670034	C	A	–	exonic	synonymous SNV	✓	

Chr, chromosome; Ref, reference base type; Alt, altered base type; SNV, single nucleotide variation.

San Diego, CA, USA). After sequencing, raw reads were processed to obtain high-quality reads by removing reads with $\geq 10\%$ unidentified nucleotides (N), reads in which $>50\%$ of bases had a Phred quality score ≤ 20 , and reads that aligned to barcode adapters. A Burrows-Wheeler Aligner approach was used to identify SNPs and InDels by aligning clear reads from each sample to the reference genome using the settings: ‘mem 4 -k 32 -M’, with $-k$ being the minimum seed length, and $-M$ being an option used to mark shorter split alignment hits as secondary alignments.¹⁸ The Genome Analysis Toolkit¹⁹ (GAT) Unified Genotyper was used for variant calling with local realignment and base quality score recalibration. The Variant Filtration tool in GAT was used to facilitate SNP

and InDel identification with appropriate settings ($-\text{Window } 4, -\text{filter } \text{“QD} < 2.0 \parallel \text{FS} > 60.0 \parallel \text{MQ} < 40.0\text{”}, -\text{G_filter } \text{“GQ} < 20\text{”}$), and variants with evidence of segregation distortion or sequencing errors were discarded. To determine the frequency of each SNP, the software tool ANNOVAR,²⁰ was used to align and annotate SNPs or InDels to the 1000 Genomes Project (<http://www.internationalgenome.org/>), HAMAP (<http://hamap.expasy.org/>), ESP6500 (<https://esp.gs.washington.edu/drupal/>), dbSNP (<https://www.ncbi.nlm.nih.gov/projects/SNP/>), and Kaviar (<http://db.systemsbio.net/kaviar/>) databases. We observed SNP mutations in certain genes in both tumor samples, with *HRAS* mutation being the most evident mutation in these samples (Table 1).



Figure 6. Follow-up photographs of Case 1. (a) Anterior and (b) lateral images of the patient after surgery.

Follow-up

We successfully followed up one of the patients (Case 1) who underwent surgery 14 years previously without further treatment. The patient's appearance was not significantly damaged, and there was no sign of recurrence (Figure 6a, b). The patient's quality of life was minimally affected, with just difficulties in eating hard food. The other patient was lost to follow-up.

Discussion

Ameloblastoma is an odontogenic tumor that is typically benign, but which may exhibit high rates of locally aggressive growth and recurrence. Although previous studies conducted in Eastern China have characterized the growth of these tumors in hundreds of patients,^{6,21} the current report describes two patients who presented with particularly large tumors (>10 cm), which had been growing for over 10 years. The unexpectedly large sizes of these tumors highlights the importance of a

prompt diagnosis and surgical removal of the ameloblastoma.

Both of the tumors reported here were solid/multicystic ameloblastoma subtype, which is the most common histological subtype of ameloblastoma. Both cases exhibited clear signs of intracellular hyalinization, which may be associated with hypoxia resulting from long-term cellular proliferation and tissue dystrophy within the tumors.^{22,23} The presence of clear cells in odontogenic tumors, including ameloblastomas, is not surprising given that they originate from the dental lamina, which includes clear cells as one of its components.²⁴ Given that clear cells have been associated with rapid tumor destruction, radical surgery with adequate tumor-free margins and close follow-up are strongly advised in patients with ameloblastoma.²⁵ Ki-67 is a well-characterized marker of cell proliferation that is often used to gauge tumor growth in clinical and research contexts.²⁶ Ki-67 staining in the present cases suggested that the ameloblastoma cells were highly proliferative, particularly in Case 2, who

was younger. CKs are characteristic epithelial cell markers, with CK7, CK8/18, and CK19 expression all being associated with certain forms of squamous cell carcinoma and with the prognosis of affected patients.^{27–29} In the current study, CK staining clearly revealed that the ameloblastoma tumors were derived from the epithelium.

Their potential for local aggressive growth means that ameloblastomas are capable of inducing significant bone destruction.³⁰ Accordingly, local bone destruction was observed in the current cases, despite both tumors being identified as benign, with no evidence of metastasis. Compared with previous reports of large ameloblastomas,^{7,31,32} we discussed their biological behaviors and possible mechanism involving EMT signaling and SNP mutation detection. We observed the phenotypic changes in the tumor cells associated with their biological behavior. EMT is a key dynamic process during which cells switch reversibly from an epithelial to a mesenchymal morphology, allowing them to migrate more effectively through the extracellular matrix.⁸ We examined the EMT characteristics of the two present ameloblastomas by assessing the tumor expression levels of N-cadherin, E-cadherin, vimentin, β -catenin, and Twist. The results confirmed that both tumors expressed EMT marker proteins, consistent with the potential for EMT to occur in ameloblastomas over time. We also conducted SNP gene sequencing to clarify the molecular basis of ameloblastoma development, by comparing SNPs in ameloblastoma and tumor-free margin tissues. This analysis identified the highest incidence of nonsynonymous SNPs in the *HRAS* gene, with evident mutations at three positions. *HRAS* mutations have also been found to function as key mediators in breast³³ and bladder cancers³⁴ and in oral squamous cell carcinoma.^{35,36} *HRAS* mutations are tightly linked to mitogen-activated protein kinase (MAPK) signaling, with the HRas-MAPK-extracellular signal-regulated

kinase signaling pathway being important for EMT regulation.^{37,38} We thus hypothesized that the observed *HRAS* mutations in these two ameloblastoma samples might be associated with their apparent EMT activity, in turn impacting the ability of these tumor cells to grow and migrate. However, further research is needed to confirm this hypothesis and to fully understand how such *HRAS* mutations impact the EMT process in ameloblastoma.

Conclusion

We report on two rare cases of very large ameloblastomas, both of which showed positive expression of EMT biomarkers and *HRAS* gene SNPs.

Patient consent

We obtained patient consent for treatment, and the patients provided written informed consent for publication.

Availability of data and material

The datasets analyzed during the current study are available from the corresponding author on reasonable request.

Acknowledgement

We thank Professor Toshinari Mikami of Iwate Medical University for reviewing and correcting the manuscript.

Declaration of conflicting interest

The authors declare that there is no conflict of interest.

Funding

The author(s) disclosed receipt of the following financial support for the research, authorship, and/or publication of this article: This work was funded by the National Natural Science Foundation of China [grant numbers 81072197, 81470758, 81972535], the Natural Science Foundation of Liaoning Province [grant number 2019-ZD-0787], and the Youth Project

Foundation of Education Department of Liaoning Province [grant number QN2019021].

ORCID iD

Ming Zhong  <https://orcid.org/0000-0001-8740-0629>

References

1. Wang GN, Zhong M, Chen Y, et al. Expression of WNT1 in ameloblastoma and its significance. *Oncol Lett* 2018; 16: 1507–1512.
2. Kim J, Nam E and Yoon S. Conservative management (marsupialization) of unicystic ameloblastoma: literature review and a case report. *Maxillofac Plast Reconstr Surg* 2017; 39: 38.
3. Speight PM and Takata T. New tumour entities in the 4th edition of the World Health Organization Classification of Head and Neck tumours: odontogenic and maxillofacial bone tumours. *Virchows Arch* 2018; 472: 331–339.
4. Lin Y, He JF, Li ZY, et al. Ameloblastoma with varied sites of metastasis: report of two cases and literature review. *J Craniomaxillofac Surg* 2014; 42: e301–e304.
5. Abiko Y, Nagayasu H, Takeshima M, et al. Ameloblastic carcinoma ex ameloblastoma: report of a case-possible involvement of CpG island hypermethylation of the p16 gene in malignant transformation. *Oral Surg Oral Med Oral Pathol Oral Radiol Endod* 2007; 103: 72–76.
6. De Roos P, Lucas C, Strijbos JH, et al. Effectiveness of a combined exercise training and home-based walking programme on physical activity compared with standard medical care in moderate COPD: a randomised controlled trial. *Physiotherapy* 2018; 104: 116–121.
7. Pramulio TH, Said HM and Kozlowski K. Huge ameloblastoma of the jaw (report of three cases). *Australas Radiol* 1985; 29: 308–310.
8. Siar CH and Ng KH. Epithelial-to-mesenchymal transition in ameloblastoma: focus on morphologically evident mesenchymal phenotypic transition. *Pathology* 2019; 51: 494–501.
9. Kurioka K, Wato M, Iseki T, et al. Differential expression of the epithelial mesenchymal transition factors Snail, Slug, Twist, TGF-beta, and E-cadherin in ameloblastoma. *Med Mol Morphol* 2017; 50: 68–75.
10. Florescu A, Margaritescu C, Simionescu CE, et al. Immunohistochemical expression of MMP-9, TIMP-2, E-cadherin and vimentin in ameloblastomas and their implication in the local aggressive behavior of these tumors. *Rom J Morphol Embryol* 2012; 53: 975–984.
11. Heikinheimo K, Kurppa KJ and Elenius K. Novel targets for the treatment of ameloblastoma. *J Dent Res* 2015; 94: 237–240.
12. Sweeney RT, McClary AC, Myers BR, et al. Identification of recurrent SMO and BRAF mutations in ameloblastomas. *Nat Genet* 2014; 46: 722–725.
13. Barnes L. *Surgical Pathology of Head and Neck*. 3rd ed. USA: CRC Press, 2008, p.23.
14. Rison RA, Kidd MR and Koch CA. The CARE (CAse REport) guidelines and the standardization of case reports. *J Med Case Rep* 2013; 7: 261.
15. CARE guidelines.[<http://www.CARE-statement.org>].
16. EQUATOR network website. [<http://www.equator-network.org>].
17. Abtahi MA, Zandi A, Razmjoo H, et al. Orbital invasion of ameloblastoma: A systematic review apropos of a rare entity. *J Curr Ophthalmol* 2018; 30: 23–34.
18. Li H and Durbin R. Fast and accurate short read alignment with Burrows-Wheeler transform. *Bioinformatics* 2009; 25: 1754–1760.
19. McKenna A, Hanna M, Banks E, et al. The Genome Analysis Toolkit: a MapReduce framework for analyzing next-generation DNA sequencing data. *Genome Res* 2010; 20: 1297–1303.
20. Wang K, Li M and Hakonarson H. ANNOVAR: functional annotation of genetic variants from high-throughput sequencing data. *Nucleic Acids Res* 2010; 38: e164.
21. Zhang X, Tian X, Hu Y, et al. Oral peripheral ameloblastoma: A retrospective series

- study of 25 cases. *Med Oral Patol Oral Cir Bucal* 2018; 23: e277–e281.
22. Hong R and Lim SC. Granular cell tumor of the cecum with extensive hyalinization and calcification: a case report. *World J Gastroenterol* 2009; 15: 3315–3318.
 23. Slootweg PJ. Bone diseases of the jaws. *Int J Dent* 2010; 2010: 702314.
 24. De Aguiar MC, Gomez RS, Silva EC, et al. Clear-cell ameloblastoma (clear-cell odontogenic carcinoma): report of a case. *Oral Surg Oral Med Oral Pathol Oral Radiol Endod* 1996; 81: 79–83.
 25. Mari A, Escutia E, Carrera M, et al. Clear cell ameloblastoma or odontogenic carcinoma. A case report. *J Craniomaxillofac Surg* 1995; 23: 387–390.
 26. Bologna-Molina R, Mosqueda-Taylor A, Molina-Frechero N, et al. Comparison of the value of PCNA and Ki-67 as markers of cell proliferation in ameloblastic tumors. *Med Oral Patol Oral Cir Bucal* 2013; 18: e174–e179.
 27. Yang ZY, Zhang HY, Wang F, et al. [Expression of cytokeratin(CK)7, CK8/18, CK19 and p40 in esophageal squamous cell carcinoma and their correlation with prognosis]. *Zhonghua Bing Li Xue Za Zhi* 2018; 47: 834–839.
 28. Zheng W, Li M, Hong Y, et al. Traditional Chinese exercise (TCE) on pulmonary rehabilitation in patients with stable chronic obstructive pulmonary disease: Protocol for a systematic review and network meta-analysis. *Medicine (Baltimore)* 2019; 98: e16299.
 29. Safadi RA, Quda BF and Hammad HM. Immunohistochemical expression of K6, K8, K16, K17, K19, maspin, syndecan-1 (CD138), alpha-SMA, and Ki-67 in ameloblastoma and ameloblastic carcinoma: diagnostic and prognostic correlations. *Oral Surg Oral Med Oral Pathol Oral Radiol* 2016; 121: 402–411.
 30. Yang Z, Li K, Liang Q, et al. Elevated hydrostatic pressure promotes ameloblastoma cell invasion through upregulation of MMP-2 and MMP-9 expression via Wnt/beta-catenin signalling. *J Oral Pathol Med* 2018; 47: 836–846. LID - 10.1111/jop.12761 [doi]. 2018.
 31. Mukhopadhyay S, Raha K and Mondal SC. Huge ameloblastoma of jaw-A case report. *Indian J Otolaryngol Head Neck Surg* 2005; 57: 247–248.
 32. Mijiti A, Ling W, Maimaiti A, et al. Single-stage management of huge desmoplastic ameloblastoma of the anterior mandible. *J Plast Reconstr Aesthet Surg* 2013; 66: 1440–1441.
 33. Myers MB, Banda M, McKim KL, et al. Breast cancer heterogeneity examined by high-sensitivity quantification of PIK3CA, KRAS, HRAS, and BRAF mutations in normal breast and ductal carcinomas. *Neoplasia* 2016; 18: 253–263.
 34. Castillo-Martin M, Collazo Lorduy A, Gladoun N, et al. H-RAS mutation is a key molecular feature of pediatric urothelial bladder cancer. A detailed report of three cases. *J Pediatr Urol* 2016; 12: 91.e1-7.
 35. Koumaki D, Kostakis G, Koumaki V, et al. Novel mutations of the HRAS gene and absence of hotspot mutations of the BRAF genes in oral squamous cell carcinoma in a Greek population. *Oncol Rep* 2012; 27: 1555–1560.
 36. Lyu H, Li M, Jiang Z, et al. Correlate the TP53 mutation and the HRAS mutation with immune signatures in head and neck squamous cell cancer. *Comput Struct Biotechnol J* 2019; 17: 1020–1030.
 37. Wong CE, Yu JS, Quigley DA, et al. Inflammation and Hras signaling control epithelial-mesenchymal transition during skin tumor progression. *Genes Dev* 2013; 27: 670–682.
 38. Qiu XY, Hu DX, Chen WQ, et al. PD-L1 confers glioblastoma multififorme malignancy via Ras binding and Ras/Erk/EMT activation. *Biochim Biophys Acta Mol Basis Dis* 2018; 1864: 1754–1769.